Effects of Targeting Endometrial Stromal Sarcoma Cells *via* Histone Deacetylase and PI3K/AKT/mTOR Signaling

PING QUAN[1], FARID MOINFAR[1,3], IRIS KUFFERATH[1], MARKUS ABSENGER[2], TATJANA KUEZNIK[2], HELMUT DENK[1], KURT ZATLOUKAL[1] and JOHANNES HAYBAECK[1]

[1]*Institute of Pathology, and* [2]*Center for Molecular Research, Medical University of Graz, Graz, Austria;*
[3]*Department of Pathology, Hospital of the Sisters of Charity Linz, Linz, Austria*

Abstract. *Aim: Endometrial stromal sarcoma (ESS) is a rare gynecological mesenchymal malignancy with only few therapeutic options. This study aimed to investigate the efficacy of the histone deacetylase (HDAC) inhibitor suberanilohydroxamic acid (SAHA) combined with inhibitors of the phosphoinositid-3-Kinase (PI3K) pathway in ESS therapy. Materials and Methods: The effects of SAHA combined with inhibitor of PI3K (LY294002, LY), mammalian target of rapamycin mTOR (rapamycin), and their combination on cell growth and the PI3K pathway in two ESS cell lines (ESS-1 and MES-SA) and one non-neoplastic cell line HESC, were investigated. Results: SAHA reduced growth of the three cell lines by inhibiting protein kinase B AKT and mTOR/p70S6K cascade activation. SAHA combined with LY or rapamycin, or both, synergistically reduced p-p70S6K and p-4E-BP1 levels. SAHA combined with LY and rapamycin led to the strongest growth inhibition and slowest growth recovery among the combination treatments. Conclusion: SAHA combined with inhibition of PI3K and mTOR could represent an efficient therapy option for patients with ESS.*

Endometrial stromal sarcoma (ESS) is a very rare mesenchymal gynecological malignancy, with an annual incidence of about 17 per million (1). ESS is divided into low-grade ESS (LES) and undifferentiated ESS (UES, including the former high-grade ESS), displaying marked differences in morphology, clinical behavior and prognosis (2). LES is a slow-growing tumor associated with an 80-100% 5-year survival rate, while UES is very aggressive,

with a 5-year survival rate of less than 25% (2-4). However, LES has a high tendency for recurrence and metastasis (4). A hallmark of malignancy is an unstable genome (5), leading to chromosomal translocation and gene fusion in sarcomas (6), *e.g.* JA zinc finger *(JAZF) 1–JJAZ1* fusion gene in ESS (7). Genomic instability can be due to defects in DNA damage response, mediated partly by post-translational modifications, *e.g.* acetylation (5). The acetylation status of core histones, essential for modulation of nucleosomal conformation and chromatin structure, is regulated by the opposing actions of histone acetyltransfererase and histone deacetylase (HDAC). Their balance is critical in controlling normal cell growth, while imbalance is associated with cancer (8). Being part of the transcriptional co-repressor complex, increased HDAC expression inhibits transcription of tumor suppressors, *e.g.* phosphatase and tensin homolog (PTEN) (9) leading to a constitutively activated phosphoinositid-3-Kinase (PI3K) pathway.

The PI3K cascade is essential for growth and survival of normal and cancerous cells. Hyperactivated protein kinase B (PKB, also known as AKT), mammalian target of rapamycin (mTOR) and eukaryotic translation initiation factor 4E-binding protein (4E-BP1) have been identified in several types of sarcomas (10-12). However, the role of the PI3K pathway in pathogenesis of ESS has not yet been addressed. Our group had observed up-regulation of HDAC2 in tissue specimens of LES and UES, and in a cognate LES cell line ESS-1 (13). A pan-HDAC inhibitor, suberanilohydroxamic acid (SAHA), induced ESS-1 cell autophagy *via* inhibition of mTOR activation, and induced apoptosis of MES-SA cells, an UES cell line, but did not affect the viability of HESC cells, a non-neoplastic human endometrial stromal cell line (14, 15). Considering the different responses to SAHA among the three cell lines, we hypothesized that SAHA affects the PI3K pathway differently in these cell lines, and its combination with inhibitors of the PI3K pathway might have synergistic anticancer effects, without markedly affecting the viability of normal cells. Therefore, we investigated the effects of SAHA alone, and in

Correspondence to: Dr. Johannes Haybaeck, Institute of Pathology, Medical University of Graz, Auenbruggerplatz 25, A-8036 Graz, Austria. Fax: +43 316384329, e-mail: johannes.haybaeck@medunigraz.at
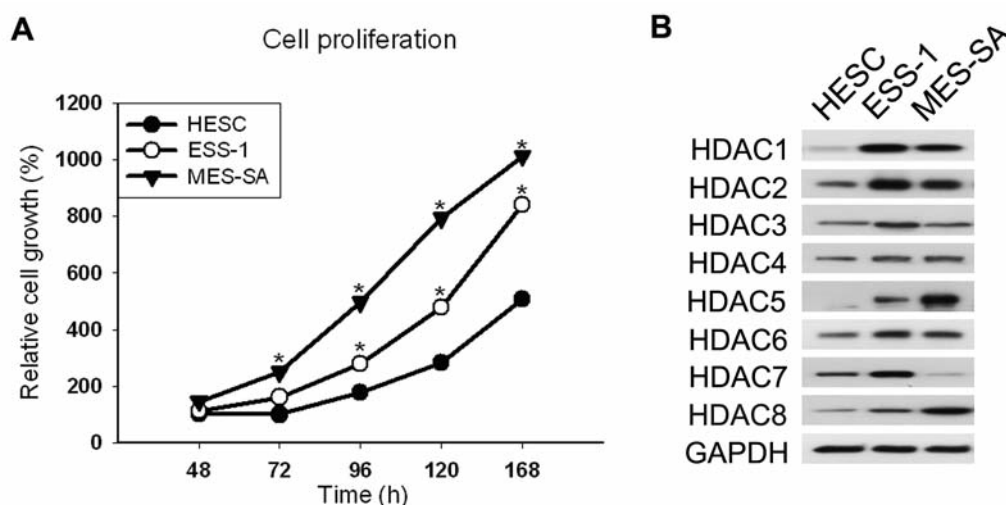
Figure 1. *Enhanced cell proliferation and HDAC expression in endometrial stromal carcomal (ESS) cell lines, compared to control HESC cells. A: Cell proliferation rates were determined for 168 h. The relative cell growth rate was normalized to that of HESC cells at 48 h, which was set to 100%. Values are presented as the mean±SD (n=3), *p<0.05 vs. HESC cells. B: Protein expression levels of class I HDAC1-3 and 8 and class II HDAC4-7 in the three cell lines were analyzed with western blot analysis. GAPDH was used as the loading control. Representative blots from two independent experiments are shown.*

combination with inhibitors of PI3K (LY294002) or mTOR (rapamycin), on the PI3K pathway and cell growth in these three cell lines.

Materials and Methods

Reagents and antibodies. SAHA (Alexis Biochemicals, Lausen, Switzerland), rapamycin and LY294002 (LY; Calbiochem, Darmstadt, Germany) were dissolved in dimethylsulfoxid (*DMSO*) and frozen at −20°C prior to use. Antibodies to the following were used: HDAC1-8, pAKT^{T308}, pAKT^{S437}, total AKT, p-p70S6K, p70S6K, p-mTOR, mTOR, PTEN, p-4EBP1, 4E-BP1, p27, glycerinaldehyd-3-phosphat-dehydrogenase (GAPDH; Cell Signaling Technology, Frankfurt, Germany), cyclin D1 and B-cell lymphoma 2 (BCL2; Dako, Vienna, Austria).

Cell culture. ESS-1 (a cognate ESS cell line), MES-SA and HESC cells (a uterine sarcoma cell line) and HESC (a non-neoplastic human endometrial stromal cell line origin from myomas) cells were used in this study. They were maintained in RPMI, Mycoy's and Dulbecco's Modified Eagle Medium/F12, respectively, supplemented with 10% fetal Calf Serum, 2 mM L-glutamine, 100 U/ml penicillin, and 100 μg/ml streptomycin (PAA, Pasching, Austria).

Cell growth and cytotoxicity assay. A total of 2×10^3 cells/well were seeded in 96-well-plates with 100 μl medium. For growth assays, cells were cultured for 168 h. For cytotoxicity assays, 48 h after plating the cells, the medium was replaced with that containing SAHA, rapamycin, LY, and their different combinations. At each time point, the plate was read at 490 nm with a spectrophotometer after 2 h incubation with 20 μl/well of CellTiter 96®Aq$_{ueous}$ One Solution (Promega, Madison, USA) at 37°C. The cells treated with the vehicle DMSO were used as control. The experiments were done in triplicate.

Western blot analysis. Cells were harvested in buffer (50 mM Tris pH 7.5, 150 mM NaCl, 1 mM EDTA, 0.1% sodium dodecyl sulfate) containing protease and phosphatase inhibitors (Roche, Vienna, Austria). Proteins were separated by polyacrylamide gel electrophoresis and transferred to nitrocellulose membrane. After incubating the membrane with the primary and corresponding secondary antibodies, specific protein bands on the membrane were visualized by ECL (Pierce, Rockford, USA).

Immunofluorescence analysis. Cells grown on cover slides were fixed in 4% paraformaldehyde, permeabilized with 0.02% Triton X-100 before incubating with primary antibody to acetylated-α-tubulin (Sigma-Aldrich, St. Louis, USA) and secondary Alexa fluor-conjugated anti-mouse antibody (Invitrogen, Carlsbad, USA). 4',6-Diamidin-2-phenylindol (DAPI) was used for nuclear staining. Epifluorescence was performed using Zeiss confocal microscopy.

Data analysis. All data were subjected to statistical analysis by an unpaired Student's *t*-test or one-way analysis of variance. A value of *p*<0.05 was considered to be significant.

Results

SAHA reduces growth of the studied cell lines with different efficacies by affecting AKT and activation of the mTOR/p70S6K cascade. ESS-1 and MES-SA cells exhibited higher cell proliferation potentials and de-regulated HDAC expression profile, compared to HESC cells (Figure 1), indicating that the cell culture model is suitable for testing the efficacy and safety of targeting HDAC in ESS.

Hrzenjak *et al.* showed that 3 μM SAHA efficiently induced death of ESS cells, but not HESC cells (14, 15). In
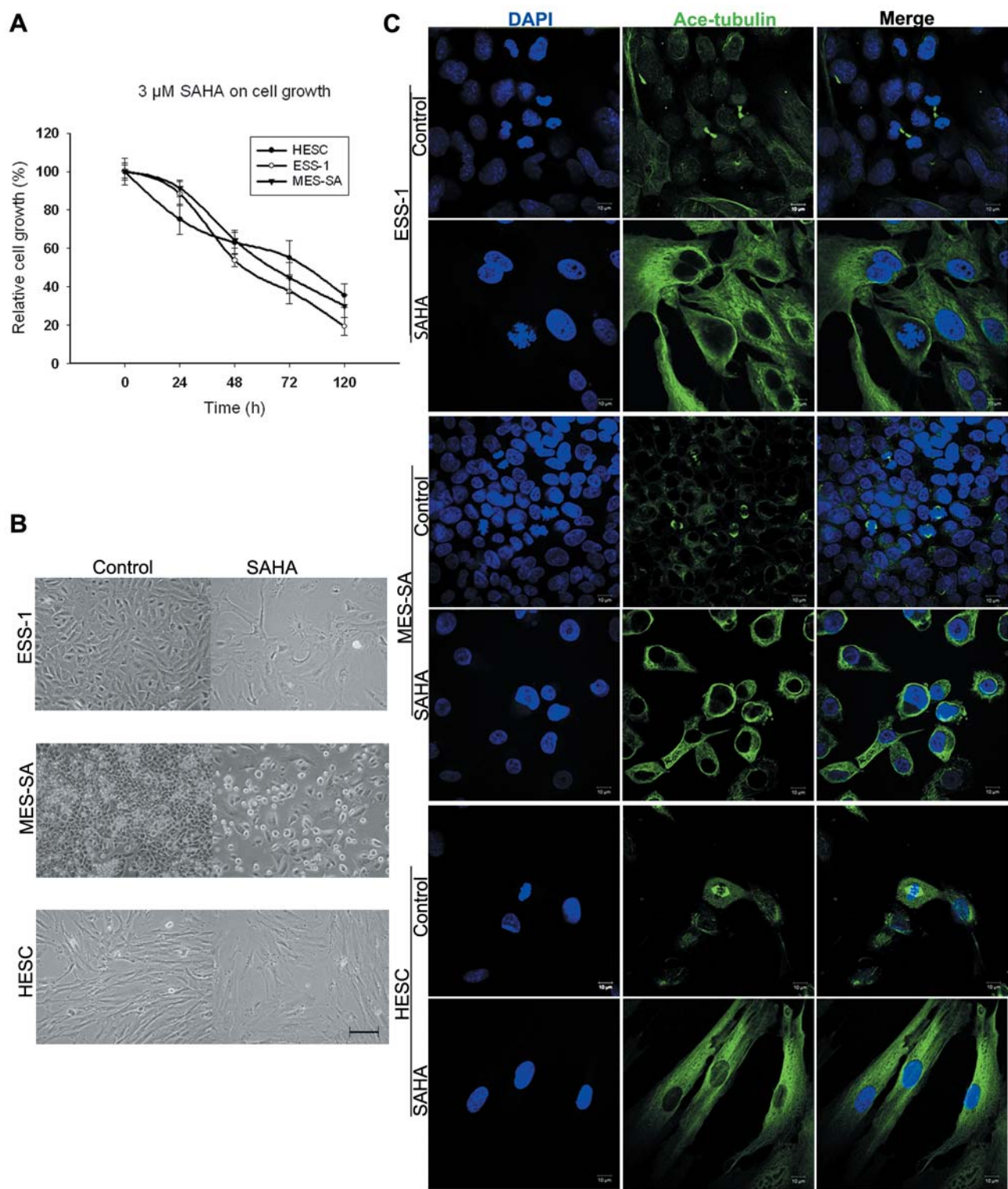
Figure 2. *SAHA reduced growth of the three cell lines with different efficacies, and induced cell death and mitosis failure in ESS cells. A: Cell growth rates were measured in cells treated with either 3 μM SAHA or vehicle (DMSO) for 120 h. The relative cell growth was normalized to that of untreated cells (set to 100% at each time point). Values are presented as the mean±SD (n=3). B: Morphological changes of cells treated with 3 μM SAHA for 72 h. Scale bar, 10 μM. C: Mitosis was visualized with immunofluorescence analysis in cells treated with 3 μM SAHA for 72 h using confocal microscopy. Cells were stained with DAPI for DNA (blue) and acetylated α-tubulin (ace-tubulin; green). Scale bars, 10 μM.*

order to elucidate if SAHA killed ESS-1 and MES-SA cells with the same efficacy, the cell growth rate was measured for 120 h (Figure 2A). SAHA at 3 μM significantly inhibited growth of both ESS cell lines in a time-dependent manner, starting at 24 h and reaching maximal effect at 120 h. Growth of MES-SA cells was less inhibited compared to ESS-1 cells. HESC cell growth was also inhibited; the effect was stronger at 24 h and less from 72 to 120 h compared to both ESS cell lines. At 120 h, SAHA reduced growth of ESS-1, MES-SA and HESC cells by about 81%, 70% and 65%, respectively, indicating different growth-inhibition efficacies.

Consistent with previous reports (14, 15), 3 μM SAHA for 72 h induced marked autophagic vacuoles in ESS-1 cells and apoptosis of MES-SA cells, but not of HESC cells (Figure 2B). HDAC inhibitors are selectively cytotoxic towards cancer cells due to mitosis failure in transformed cells but not in differentiated cells (16). During mitosis acetylated α-tubulin accumulates in spindle microtubules (17). SAHA increased acetylated α-tubulin by inhibiting HDAC6, a class II HDAC that specifically deacetylates α-tubulin (18). Thus we visualized mitosis by immunostaining with an antibody against acetylated α-tubulin (Figure 2C). In untreated cells, acetylated α-tubulin was only enriched in the spindle. In contrast, SAHA strongly increased cytoplasmic acetylated α-tubulin in all cell lines, and mitosis was not seen in cells upon 72 h treatment (Figure 2C). Marked mitosis failure or cell death was observed in ESS cells but not in HESC cells. Mitotic catastrophe, *e.g.* DNA bridging and multiple nuclei, was identified in ESS-1 cells. Apoptotic bodies and condensed nuclei were detected in MES-SA cells (Figure 2C). Thus, SAHA reduced the growth of the three cell lines by inhibiting mitosis, but induced ESS cell death *via* mitosis failure or apoptosis.

Despite the undefined role of tubulin acetylation in mitosis, overexpression of acetylated α-tubulin has no effect on cell morphology (17). Thus, mitosis failure in ESS cells cannot be ascribed solely to increased acetylated α-tubulin expression, but must be also due to molecular changes involved in cell growth and survival. Alterations in the PI3K/AKT/mTOR pathway, p27, cyclin-D1 and BCL2 protein levels were determined in cells treated with SAHA for 72 h (Figure 3). SAHA reduced p-4E-BP1 protein levels in all cell lines. In ESS-1 cells, SAHA strongly reduced pAKT^{S437}, pAKT^{T308}, p-mTOR and p-p70S6K levels at 24, 48 and 72 h. In MES-SA cells, SAHA did not significantly reduce p-mTOR and p-p70S6K levels at 72 h, but did increase pAKT^{S437} and pAKT^{T308} levels after 48 h. In HESC cells, pAKT^{S437} and pAKT^{T308} levels were significantly reduced at 24 h, but slightly increased at 48 h, and almost reached the levels of untreated cells at 72 h. p-mTOR and p-p70S6K levels in HESC cells were also not markedly affected by SAHA. p27 and cyclin-D1 protein

levels were differentially affected in the three cell lines in response to SAHA. SAHA increased the p27 level in ESS-1 and HESC cells at 24 and 48 h, but not in MES-SA cells up to 72 h. Cyclin-D1 protein level was reduced in HESC cells, but increased in ESS-1 and MES-SA cells for all time intervals. Additionally, BCL2 levels in both ESS cell lines were strongly reduced by SAHA during 72 h, while being undetectable in HESC cells.

Molecular changes and cell growth were further examined in the three cell lines with increasing doses of SAHA for 72 h (Figure 4), showing that different growth-inhibition efficacies of SAHA among the three cell lines were consistently accompanied by different changes in pAKT, p-mTOR and p-p70S6K. An overview of the effects of SAHA on the three cell lines is shown in Table I.

In order to determine if the co-inhibition of AKT and of mTOR cascade activation could improve SAHA efficacy, the three cell lines were treated with LY or rapamycin in combination with SAHA.

SAHA combined with LY additively inhibits the AKT/p70S6K/4E-BP1 cascade and growth in the studied cell lines. The molecular effects of SAHA combined with 5 or 10 μM LY were determined in both ESS cell lines after 72 h (Figure 5A). Several molecular changes were induced in a LY-dose-dependent manner. Levels of pAKT^{S437}, p-mTOR, p-p70S6K and p-4E-BP1 were synergistically reduced to the lowest in both ESS cell lines; pAKT^{T308} level decreased and the p27 level was increased in ESS-1 cells. The combination also reduced possible adverse side-effects of each drug alone. For instance, LY reduced SAHA-induced up-regulation of pAKT^{T308} in MES-SA cells. SAHA abolished p21 down-regulation, and blocked increased expression of BCL2 caused by LY in both ESS cell lines (Figure 5A).

In HESC cells, lowered pAKT levels were restored after 72 h of SAHA treatment (Figure 3). In order to examine this effect upon co-treatment, HESC cells were treated with SAHA combined with 5 or 10 μM of LY for 48 and 72 h (Figure 5A). p-mTOR, p-p70S6K and p-4E-BP1 levels were reduced, and p27 levels were increased at 48 and 72 h. Up-regulation of pAKT^{T308} and pAKT^{S437} caused by LY were reduced to lower levels than with each drug alone. However, levels of p-p70S6K, but not pAKT were partly restored with increasing duration of treatment.

Corresponding to the molecular changes, SAHA combined with LY inhibited growth of the two ESS cell lines in a LY dose-dependent manner (Figure 5B and C). Obvious growth inhibition appeared at 48 h, and reached its maximum at 120 h. From 48 to 72 h, growth inhibition was stronger than on treatment with SAHA alone, but from 120 to 168 h was similar to that with SAHA due to strong cytotoxicity of SAHA. SAHA combined with LY still caused marked cell death of ESS cells, but not of HESC cells (data not shown).
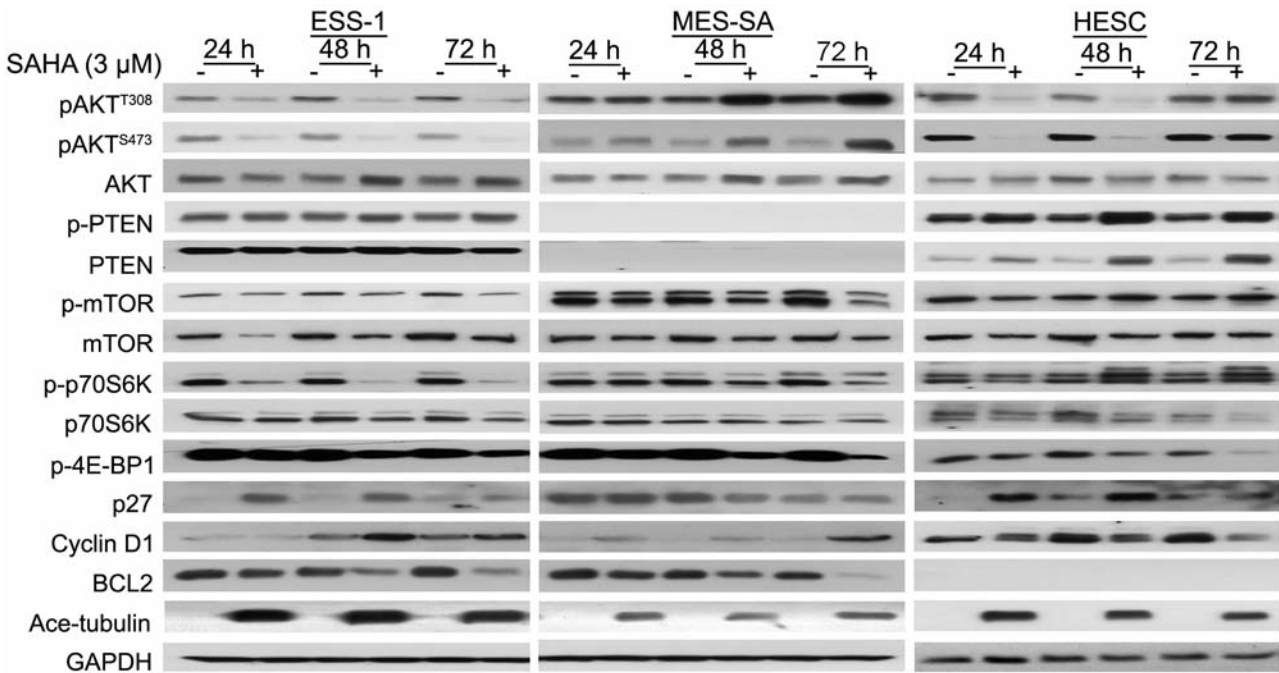
Figure 3. *Effects of SAHA on the PI3K pathway, cell-cycle regulators and BCL2 protein in cells were analyzed with western blot analysis in ESS-1, MES-SA and HESC cells treated with 3 μM SAHA for 72 h, respectively. GAPDH was used as a loading control.*

However, this combination inhibited HESC cell growth more than either SAHA or LY alone in a LY-dose-dependent manner (Figure 5D). The comparison of the growth-inhibition efficiency showed no significant differences among the three cell lines treated with SAHA combined with LY for 72 h (Figure 5E), indicating a non-selective action on ESS cells. A summary of the effects of SAHA combined with LY on the three cell lines is shown in Table II.

SAHA combined with rapamycin reduces p-p70S6K/p-4E-BP1 and cell growth in three cell lines. The molecular effects of SAHA combined with 10 and 200 nM rapamycin are shown in Figure 6A. Similar to the combination of SAHA with LY, SAHA combined with rapamycin additively reduced p-mTOR, p-p70S6K, and p-4E-BP1 levels, but restored p21 expression which was down-regulated by rapamycin in both ESS cell lines. It reversed the reduction of p27 and increase of BCL2 caused by rapamycin in ESS-1 cells, and in MES-SA cells, partially reversed up-regulation of BCL2 caused by rapamycin, but did not affect the level of p27. Changes in pAKT^{T308} and pAKT^{S437} levels consistently differed between the two ESS cell lines (Figure 6A). In ESS-1 cells, the up-regulation of pAKT^{T308} and pAKT^{S437} caused by rapamycin was reduced by SAHA combined with rapamycin (Figure 6A). In MES-SA cells, SAHA combined with rapamycin reduced pAKT^{S437} more, but increased pAKT^{T308} more than

SAHA or rapamycin alone in a rapamycin dose-dependent manner, *i.e.* the lowest pAKT^{S437} and highest pAKT^{T308} levels were found in cells treated with SAHA plus 200 nM rapamycin. In HESC cells, levels of p-mTOR, p-p70S6K and p-4E-BP1 were significantly reduced at 48 h, but slightly

Table I. Effects *of SAHA on the three cell lines used in this study.*

Effect on	Cell line		
	ESS-1	MES-SA	HESC
pAKT^{T308}	↓	↑	↓↑
pAKT^{S437}	↓	↑	↓↑
AKT	↑	↑	–
p-mTOR	↓↓	–	–
mTOR	↓	–	–
p-p70S6K	↓	–	–
p-4E-BP1	↓	↓	↓
P27	↑	–	↑
Cyclin-D1	↑	↑	↓
BCL2	↓	↓↓	Undetected
Cell viability	↓	↓	–
Cell growth	↓↓↓	↓↓	↓

Note: Effects of SAHA on cells were compared with those of cells treated with the vehicle DMSO. ↑: increased; ↓: reduced; –: no significant change; ↑↓: first reduced, then increased.
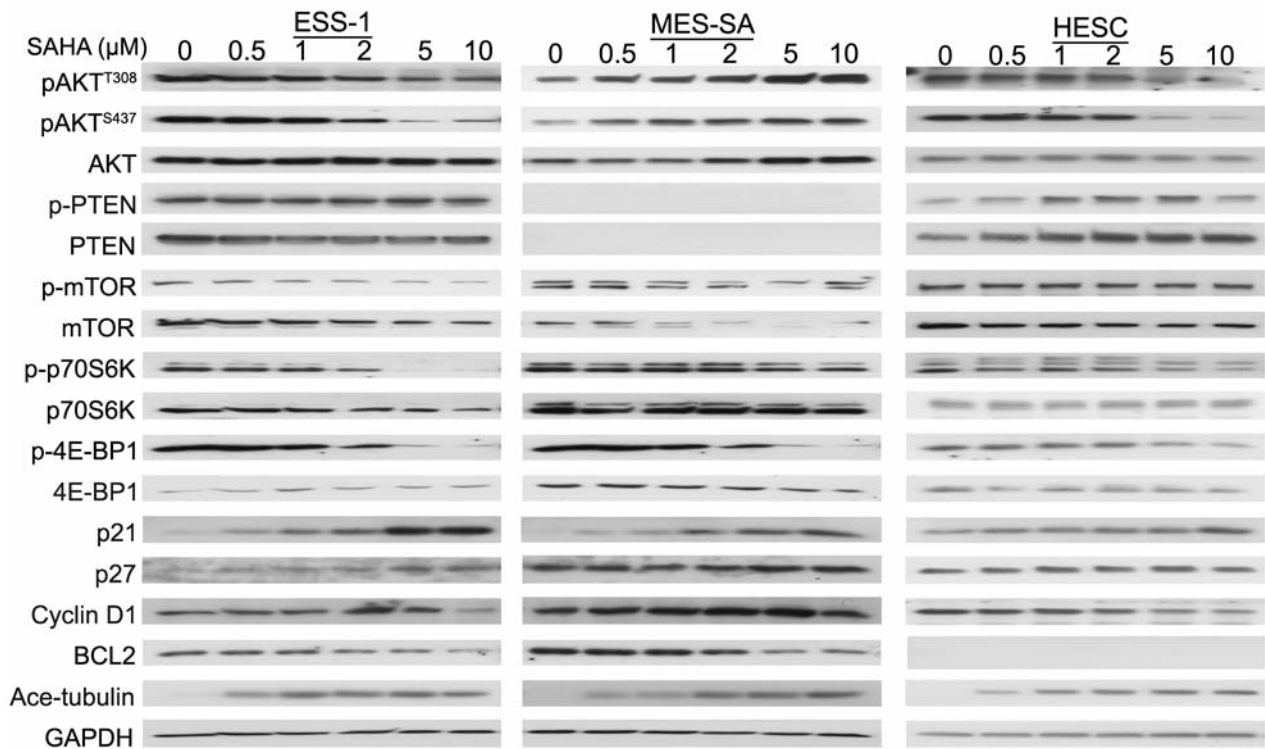
Figure 4. *Dose-effects of SAHA on the PI3K pathway and cell growth in the three cell lines. Molecular changes in the PI3K pathway and cell-cycle regulators were analyzed with western blot analysis in ESS-1, MES-SA and HESC cells treated with increasing doses of SAHA for 72 h. GAPDH was used as a loading control.*

increased at 72 h (Figure 6A). Reduction of pAKT^{T308} and pAKT^{S437} levels caused by SAHA were restored by SAHA combined with rapamycin in a time-dependent manner.

Cell growth rates were determined in cells treated with SAHA combined with 10 or 200 nM rapamycin for 168 h (Figure 6B-D). Despite some rapamycin dose-dependent differences among the three cell lines, this combination treatment induced earlier and stronger growth inhibition in our cell lines than each drug alone. SAHA combined with 10 nM rapamycin inhibited ESS-1 cell growth less than with 200 nM rapamycin during 168 h (Figure 6B). However, SAHA combined with 10 nM rapamycin inhibited MES-SA cell growth more than with 200 nM rapamycin (Figure 6C). In HESC cells, SAHA combined with 10 nM rapamycin led to a growth-inhibition efficiency equal to that with 200 nM rapamycin (Figure 6D). Microscopic observations showed that SAHA combined with rapamycin caused cell death in both ESS cell lines, but not in HESC cells (data not shown). At 72 h, SAHA combined with either 10 or 200 nM rapamycin inhibited growth of ESS cells more than that of HESC cells, indicating a selective inhibitory action in ESS cells (Figure 6E). A summary of effects of SAHA combined with rapamycin on the three cell lines is shown in Table III.

SAHA combined with PI3K and mTOR inhibitor, but not with PI3K inhibitor, was shown to strongly reduce tumor growth *in vivo* in a mouse model (19). Therefore the effects of SAHA combined with LY and rapamycin were tested on our cell lines.

SAHA combined with PI3K and mTOR inhibitors reduces p-p70S6K/p-4E-BP1 and cell growth to the lowest levels in three cell lines. Synergistic molecular changes were seen in cells treated with SAHA combined with LY and rapamycin for 72 h (Figure 7A). This triple combination treatment strongly reduced pAKT^{S437}, p-p70S6K and p-4E-BP1 levels in the three cell lines, and pAKT^{T308} levels in ESS-1 and HESC cells. In particular, levels of pAKT^{S437} and p-4E-BP1 in all cell lines, p-p70S6K in ESS-1 and HESC cells, and pAKT^{T308} in ESS-1 cells were reduced to the lowest among all treatments. Up-regulation of pAKT^{T308} level induced by SAHA and rapamycin in MES-SA cells was reduced to the level of untreated cells. Moreover, SAHA combined with LY and rapamycin strongly increased p27 protein level in all cell lines, and p21 level in both ESS cell lines, but did not affect p21 in HESC cells (Figure 7A).

Table II. *Effect of SAHA combined with LY294002 (LY) on the three cell lines used in this study.*

	Cell line								
	ESS-1			MES-SA			HESC		
Effect on	SAHA	LY	SAHA/LY	SAHA	LY	SAHA/LY	SAHA	LY	SAHA/LY
pAKTT^{308}	↓	↓	↓↓	↑	↓	↓	↓	↑	↓
pAKTS^{437}	↓	↓	↓↓	↑	↓	↓	↓	↑	↓
AKT	↑	↑	↑	↑	↑↑	↑	–	–	–
p-mTOR	↓	↓	↓	–	–	↓	–	–	↓
mTOR	↓	–	–	–	–	↓	–	–	–
p-p70S6K	↓	↓↓	↓↓↓	–	↓	↓↓	↓	↓	↓↓
p-4E-BP1	↓	↓	↓↓	↓	↓	↓	↓	↓	↓↓
P21	↑	↓	↑	↑	↓	↑↑	↑	↑	–
P27	↑	↑	↑	↑	↑	↑	↑	↑	↑
Cyclin D1	↑	↑	–	↑	–	↑↑	↓	–	↓
BCL2	↓	↑	–	↓	↑	–	Undetected		
Cell viability	↓	–	↓	↓	–	↓	–	–	–
Cell growth	↓	↓	↓↓	↓	↓	↓↓	↓	↓	↓↓

Note: Effects of SAHA combined with LY (SAHA/LY) on cells were compared with those of cells treated with the vehicle DMSO. ↑: Increased; ↓: reduced; −: no significant change.

Table III. *Effect of SAHA combined with rapamycin (Ra) on the three cell lines used in this study.*

	Cell line								
	ESS-1			MES-SA			HESC		
Effect on	SAHA	Ra	SAHA/Ra	SAHA	Ra	SAHA/Ra	SAHA	Ra	SAHA/Ra
pAKTT^{308}	↓	↑	–	↑	↑	↑	↓	↑↑	↑
pAKTS^{437}	↓	↑	↓	↑	↓	↓↓	↓	↑↑	↑
AKT	↑	↑	↑↑	↑	↑	↑↑	–	–	–
p-mTOR	↓	↓	↓↓	–	–	↓↓	–	↓	↓
mTOR	↓	↓	↓↓	–	–	–	–	–	–
p-p70S6K	↓	↓↓	↓↓	–	↓	↓↓	–	↓	↓
p-4E-BP1	↓	↓	↓↓	↓	↓	↓↓	↓	↓	↓
P21	↑	↓	↑	↑	↓	↑	↑	↑	↑
P27	↑	–	↑	↑	↑	↑	↑	↑	↑
Cyclin D1	↑	↑	↑	↑	↑	↑	↓	–	↓
BCL2	↓	↑	↓	↓	↑	↑	Undetected		
Cell viability	↓	–	↓	↓	–	↓↓	–	–	–
Cell growth	↓	↓	↓↓	↓	↓	↓↓	↓↓	↓	↓↓↓

Note: Effects of SAHA combined with rapamycin (SAHA/Ra) were compared with those of cells treated with the vehicle DMSO. ↑: Increased; ↓: reduced; −: no significant change.

Cell growth was determined in cells treated with SAHA combined with LY and rapamycin for 168 h (Figure 7B-D). In ESS-1 cells, from 24 to 72 h this triple-combination treatment induced the earliest and strongest growth inhibition (30-75%) among all treatments, while from 120 to 168 h, it induced growth inhibition equal to that of SAHA with rapamycin (both 83% at 168 h). From 24 to 168 h, the inhibition efficacy of SAHA-alone was increased from 4 to 73%. At 168 h, it was only lower than that of SAHA combined with LY and rapamycin, or SAHA combined with rapamycin, suggesting that SAHA-alone is also effective in targeting ESS (Figure 7B).

Because rapamycin inhibited MES-SA cell growth more efficiently at lower doses than at higher doses, it was applied to MES-SA cells at concentrations of 5, 10 and 200 nM (Figure 7C). Consistently, SAHA and LY combined with 5
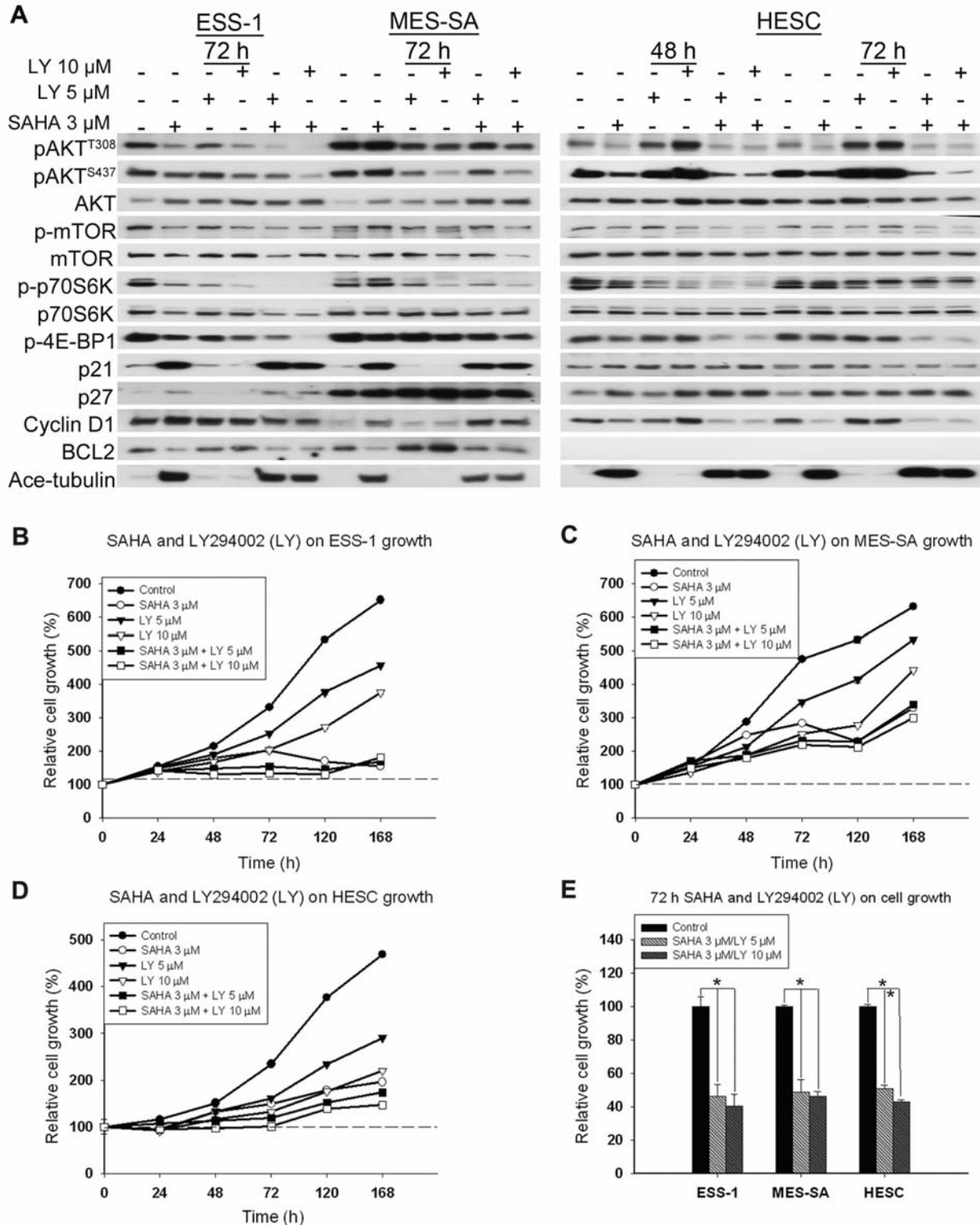
Figure 5. *SAHA combined with the PI3K inhibitor LY294002 (LY) additively reduced activation of the PI3K pathway and cell growth. A: Western blot analysis of changes in the PI3K pathway and cell-cycle regulators in ESS-1 and MES-SA and HESC cells upon 3 μM SAHA combined with 5 or 10 μM LY for 72 h. GAPDH was used as a loading control. Growth/viability of ESS-1 (B), MES-SA (C) and HESC (D) cells treated with 3 μM SAHA together with 5 or 10 μM LY was determined for 168 h. The relative cell growth was normalized with that of untreated cells at 0 h (set to 100%). Values are presented as the mean±SD (n=3). E: Growth of the three cell lines upon co-treatment of SAHA with LY for 72 h was compared with that of untreated cells (set to 100%). Values are presented as the mean±SD (n=3), *p<0.05 vs. untreated cells.*
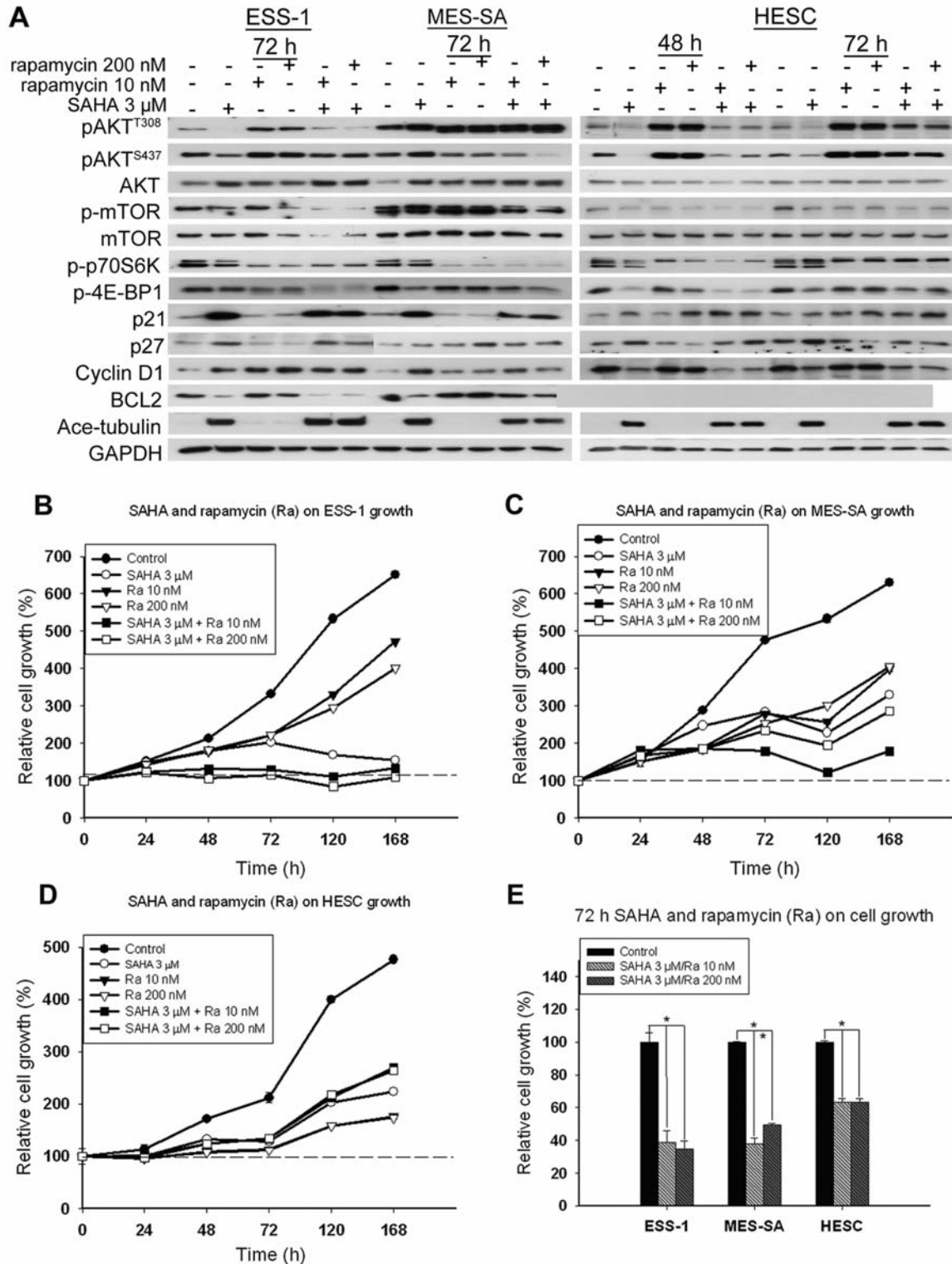
Figure 6. *SAHA combined with the mTOR inhibitor rapamycin additively inhibited activation of p70S6K and 4E-BP1, and cell growth in the three cell lines. A: Western blot analysis of changes in the PI3K pathway and cell-cycle regulators in ESS-1, MES-SA and HESC cells upon 3 μM SAHA combined with 10 or 200 nM rapamycin for 72 h. GAPDH was used as a loading control. Growth/viability of ESS-1 (B), MES-SA (C) and HESC (D) cells treated with 3 μM SAHA combined with 10 or 200 nM rapamycin for 168 h was determined. The relative cell growth was normalized to that of untreated cell at 0 h, which was set to 100%. Values are presented as the mean±SD (n=3). E: Growth of the three cell lines upon the co-treatment of SAHA with rapamycin for 72 h was compared with that of untreated cells (set to 100%). Values are presented as the mean±SD (n=3), *p<0.05 vs. untreated cells.*
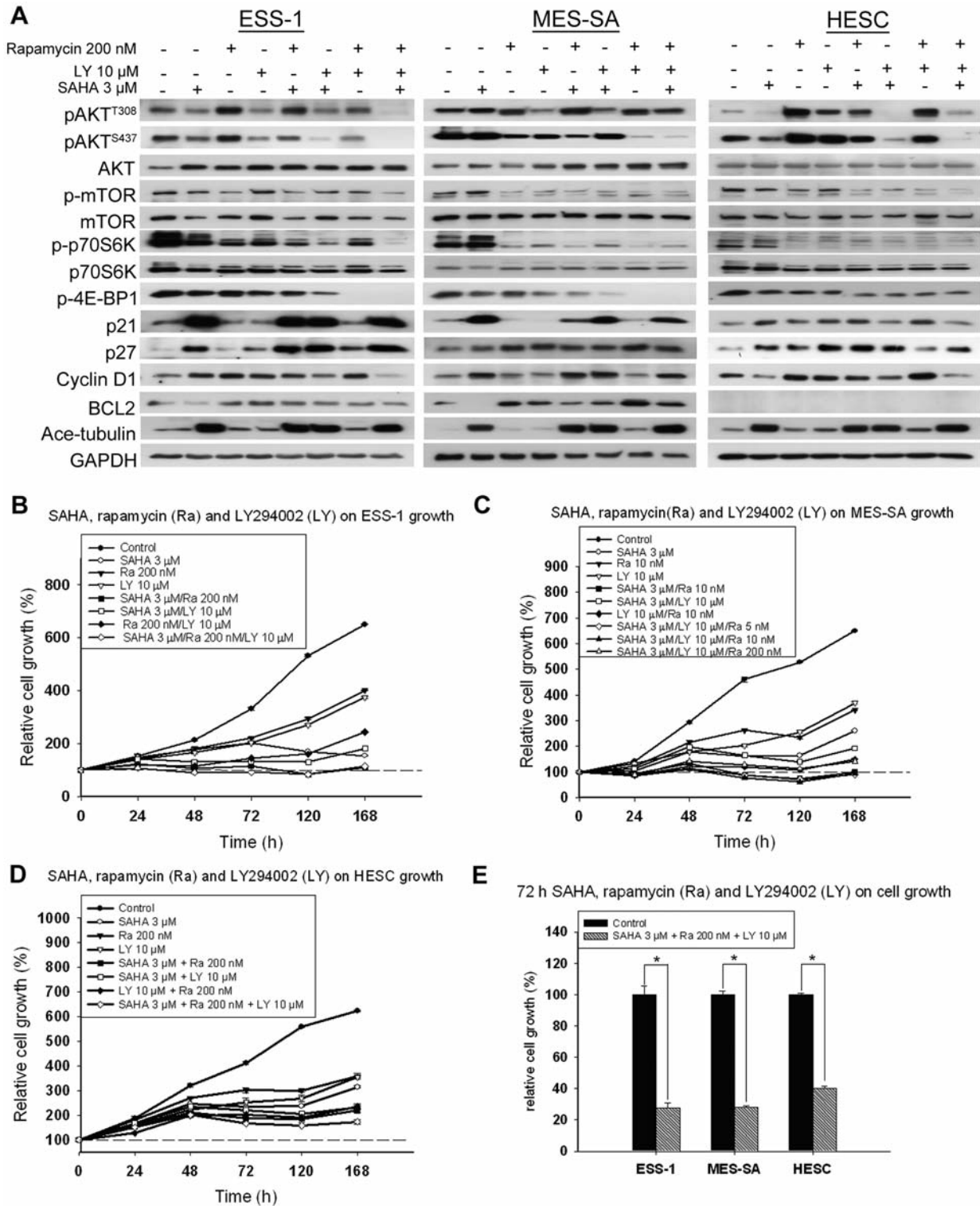
Figure 7. *SAHA combined with rapamycin and LY additively inhibited activation of p70S6K and 4E-BP1 and cell growth of the three cell lines. A: Western blot analysis of changes in the PI3K pathway and cell-cycle regulators in ESS-1, MES-SA and HESC cells treated with 3 μM SAHA together with 200 nM rapamycin and 10 μM LY for 72 h. GAPDH was used as a loading control. Growth/viability of ESS-1 (B), MES-SA (C) and HESC (D) cells with 3 μM SAHA combined with 10 or 200 nM rapamycin and 10 μM LY for 168 h was determined. The relative cell growth was normalized to that of untreated cells at 0 h (set to 100%). Values are presented as the mean±SD (n=3). E: Growth of the three cell lines upon the co-treatment of SAHA with rapamycin and 10 μM LY for 72 h was compared with that of untreated cells (set to 100%). Values are presented as the mean±SD (n=3), *p<0.05 vs. untreated cells.*
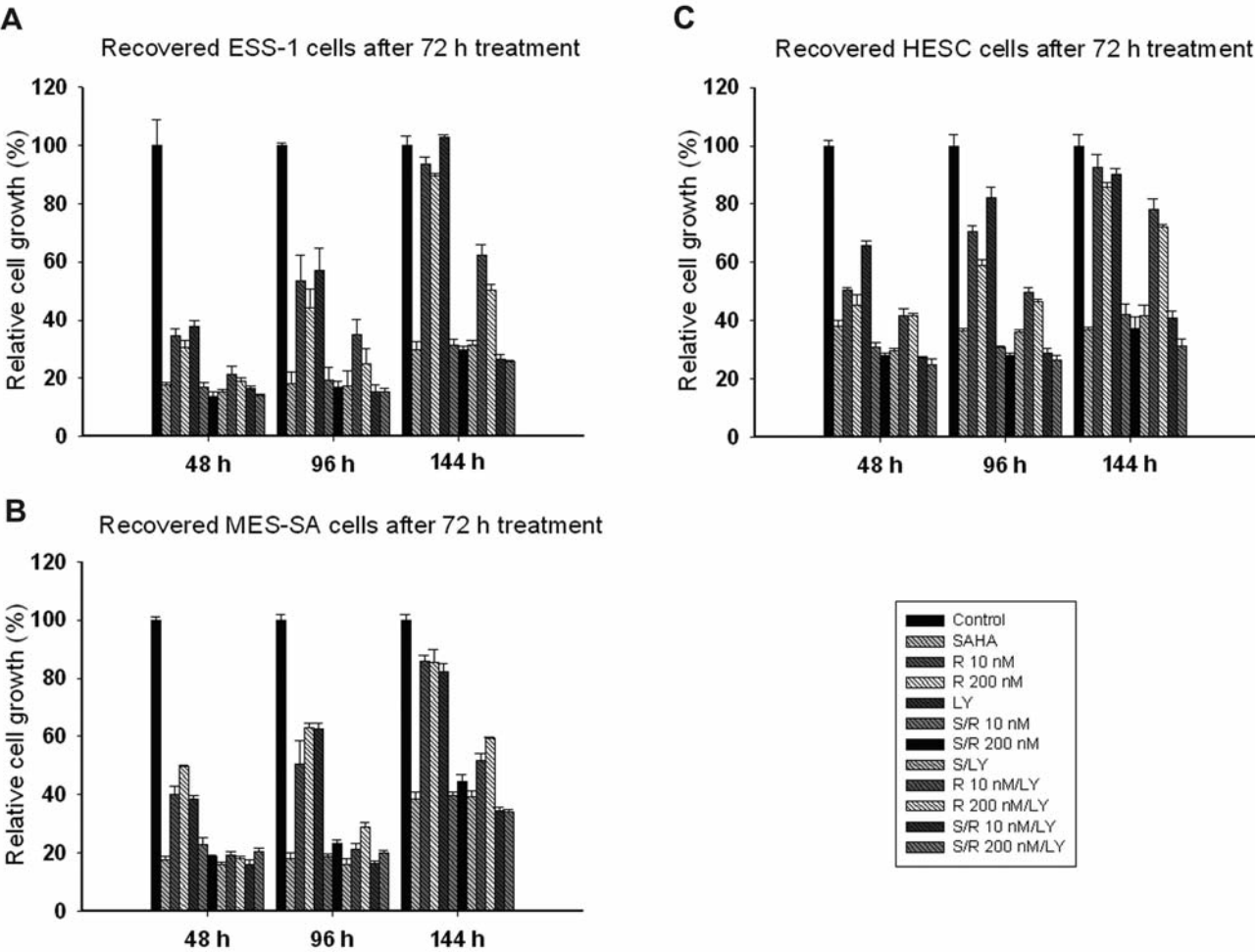
Figure 8. *Delayed cell recovery by SAHA alone or combined with rapamycin (Ra) and LY294002 (LY). ESS-1 (A), MES-SA (B) and HESC (C) cells were treated with SAHA, Ra, LY alone or their different combinations for 72 h, then replaced with the medium without drugs for 48, 96 and 144 h. The relative growth of recovered cells was normalized to that of untreated cells, which were set to 100%. Values are presented as the mean±SD (n=3).*
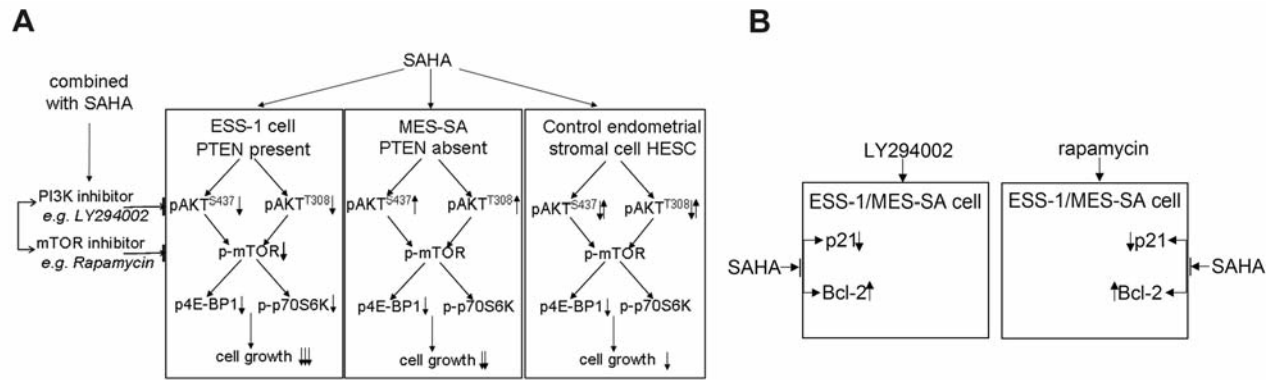
Figure 9. *Schematic illustration of the rationale of treatment with SAHA combined with the inhibitors of PI3K and mTOR. A: SAHA differently affects activation of AKT and the mTOR/p70S6K cascade, in turn leading to different growth inhibition efficacies in the three cell lines dependent on their PTEN level and molecular profile. The inhibitors of PI3K or mTOR with SAHA synergistically reduced ESS cell growth via reduction of activation of AKT and the mTOR/p70S6K cascade. B: Inhibitor of PI3K (LY294002) or mTOR (rapamycin) reduced p21, but increased BCL2 levels. These side-effects might promote cell survival, which might be abrogated by the combination with SAHA.*

or 10 nM rapamycin induced stronger growth inhibition than with 200 nM rapamycin. Like in ESS-1 cells, SAHA and LY combined with 10 nM rapamycin inhibited MES-SA cell growth (87%) similar to that of SAHA combined with 10 nM rapamycin (85%). However, SAHA and LY combined with 200 nM rapamycin reduced MES-SA cell growth (79%) to a similar extent as LY combined with rapamycin at any dose (77%), being stronger than other treatments during 168 h. Therefore, better responses of MES-SA cells to SAHA or LY combined with rapamycin, particularly at low doses, suggesting that rapamycin acts as an important modulator in improving SAHA or LY efficiency.

The triple combination inhibited HESC cell growth to the greatest extent from 48 to 168 h, compared to other treatments (Figure 7D). No cell death was detected in HESC cells with any treatment, in contrast to marked ESS cell death (data not shown). Additionally, at 72 h SAHA combined with LY and rapamycin reduced growth of both ESS cell lines more than that of HESC cells, indicating a selective inhibitory action in ESS cells (Figure 7E).

Therefore, SAHA in combination with LY and rapamycin induced the strongest inhibition of the PI3K/AKT/mTOR pathway and ESS cell growth compared to other treatment options. However, considering the fact that SAHA combined with rapamycin reduced ESS cell growth similar to SAHA combined with LY and rapamycin, but was less cytotoxic to HESC cells, the best therapeutic strategy remains unclear. In addition to cancer growth reduction, an optimal therapy option should maintain a disease-free period or stable disease as long as possible. Therefore, the number of cells recovering was monitored for 144 h after 72 h of treatments, showing the slowest growth recovery in both ESS cell lines treated with SAHA combined with LY and rapamycin, followed by those with SAHA-alone (Figure 8), suggesting that SAHA combined with inhibition of PI3K and mTOR is efficient in the treatment of ESS, and SAHA alone also presents a promising therapeutic option. A comparison of effects of combination treatments on the three cell lines shown in Table IV.

Discussion

In the present study, effects of inhibitors of HDAC (SAHA), PI3K (LY294002, LY) and mTOR (rapamycin) alone and in combination, on two different ESS cell lines and one control cell line were investigated.

HDAC inhibitors induce growth arrest in normal and cancer cells by modulating expression of tumor-suppressor genes and cell cycle regulators (16), and preferentially cause cancer cell death by regulating pro-apoptotic and anti-apoptotic proteins (8). We showed that SAHA reduced growth of ESS cell with higher efficacies than that of control cells, and induced mitotic failure and death of ESS cells, confirming its high efficiency and specificity in ESS therapy.

ESS cell death was due to reduced BCL2 expression, while growth inhibition was related to changes in the cell-cycle regulators p21, p27, and in the PI3K pathway, particularly AKT activation. SAHA reduced AKT phosphorylation in ESS-1, but increased it in MES-SA cells, corresponding to its higher efficacy in ESS-1 than in MES-SA cells. Interestingly, AKT phosphorylation in HESC cells was initially reduced, but then recovered, even in the presence of SAHA. Although SAHA has been used in patients with cutaneous T-cell lymphoma, there was only a 30% response rate. SAHA efficiency was also not promising in other clinical trials (20). Several mechanisms were suggested for SAHA resistance, including constitutively activated Janus kinase/signal transducers pathway and oxidative stress resistance (21). Different AKT activation patterns might be an alternative mechanism in modulating SAHA efficiency.

Effects of SAHA on AKT activation may be related to the PTEN level. AKT activation was enhanced in MES-SA cells with PTEN deficiency, but reduced in ESS-1 cells with a PTEN level comparable to that of HESC cells. PTEN loss leads to uncontrolled phosphatidylinositol-triphosphate production (22), which may contribute to SAHA-induced AKT activation in MES-SA cells. Cancer cells with PTEN loss have been shown to be resistant to usual chemotherapy (23). Patients with PTEN-deficient breast cancer poorly respond to trastuzumab since trastuzumab inhibits the PI3K pathway *via* increasing PTEN membrane location and phosphatase activity (24). PTEN loss has been found in endometrial cancer and leiomyosarcoma (25). It occurs *via* different ways, *e.g.* genetic mutations, epigenetic silencing, and loss of heterozygosity (26). Loss of heterozygous PTEN was found in 37% of ESS cases (27). However, the role of PTEN in ESS pathogenesis and in SAHA-induced AKT activation needed to be investigated further.

Targeting the PI3K pathway has shown high anticancer efficiency (28). Some types of sarcomas respond to the PI3K inhibition (29). We have shown that inhibitors of PI3K (LY) and mTOR (rapamycin) reduced ESS cell growth, providing the first evidence of targeting the PI3K pathway in ESS. As a pan-PI3K inhibitor, LY is a useful tool for identifying the role of PI3K in cancer (28), although it is unstable and thus unsuitable for direct application to patients. Complete inhibition of the PI3K/AKT/mTOR pathway by LY in ESS cells indicated that LY effects were independent of PTEN level and that the class I PI3K was the main regulator of this pathway in ESS cells, in line with previous reports (30). In HESC cells, LY blocked p70S6K and 4E-BP1 activation, but increased AKT activation at both phosphorylation sites, suggesting that LY affected normal cells in a way different from ESS cells. AKT activation caused by LY might be due to a negative feedback from p70S6K or *via* an alternative mechanism. For example, the PI3K expression profile in HESC cells might be different from that in ESS cells because

Table IV. *Comparison of effects of different combination treatments on the three cell lines used in this study.*

	ESS-1						
Effect on	SAHA	Ra	LY	SAHA/Ra	SAHA/LY	Ra/LY	SAHA/Ra/LY
pAKT^{T308}	↓	↑↑	↓	-	↓↓	–	↓↓
pAKT^{S437}	↓	↑	↓	↓	↓↓	↓	↓↓↓
AKT	↑	↑	↑	↑	↑	↑	↑
p-mTOR	↓	↓	↓	↓↓	↓	↓	↓↓
mTOR	↓	↓	–	↓↓	–	↓	↓
p-p70S6K	↓	↓↓	↓↓	↓↓	↓↓↓	↓	↓↓↓↓
p-4E-BP1	↓	↓	↓	↓	↓↓	↓↓↓	↓↓↓
P21	↑	↓	↓	↑	↑	–	↑
P27	↑↑	–	↑	↑↑	↑↑	↑	↑↑
Cyclin D1	↑↑	↑↑	↑↑	↑	–	↑↑	↓
BCL2	↓	↑	↑	–	–	–	–
Cell viability	↓	–	–	↓	↓	–	↓
Cell growth	↓	↓	↓	↓↓	↓↓	↓	↓↓↓
Growth recovery	↓↓↓↓	↓	↓	↓↓↓	↓↓↓	↓↓	↓↓↓↓

	MES-SA						
Effect on	SAHA	Ra	LY	SAHA/Ra	SAHA/LY	Ra/LY	SAHA/Ra/LY
pAKT^{T308}	↑	↑	↓	↑	↓	↑	–
pAKT^{S437}	↑	↓	↓	↓↓	↓	↓↓↓	↓↓↓
AKT	↑	↑	↑↑	↑↑	↑	↑	↑
p-mTOR	–	–	–	↓↓	↓	↓	↓
mTOR	–	–	–	–	↓	–	–
p-p70S6K	–	↓	↓	↓↓	↓↓	↓↓	↓↓
p-4E-BP1	↓	↓	↓	↓↓	↓	↓↓↓	↓↓↓
P21	↑	↓	↓	↑	↑↑	–	↑↑
P27	↑	↑	↑	↑	↑	↑	↑
Cyclin D1	↑	↑	–	↑	↑↑	–	↑
BCL2	↓	↑	↑	↑	↑	↑↑	↑
Cell viability	↓	–	–	↓↓	↓	–	↓
Cell growth	↓	↓	↓	↓↓	↓↓	↓	↓↓↓
Growth recovery	↓↓↓↓	↓	↓	↓↓↓	↓↓↓	↓↓	↓↓↓↓

	HESC						
Effect on	SAHA	Ra	LY	SAHA/Ra	SAHA/LY	Ra/LY	SAHA/Ra/LY
pAKT^{T308}	↓	↑↑	↑	↑	↓↓	↑↑	–
pAKT^{S437}	↓	↑↑	↑↑	↑	↓↓	↑	↓↓
AKT	–	–	–	–	–	–	–
p-mTOR	–	↓	–	↓↓	↓↓	↓↓	↓↓
mTOR	–	–	–	–	–	–	–
p-p70S6K	–	↓	↓	↓	↓	↓	↓
p-4E-BP1	↓	↓	↓	↓	↓↓	↓↓↓	↓↓↓
P21	↑	↑	↑	↑	–	↑	–
P27	↑	↑	↑	↑↑	↑↑	↑	↑↑
Cyclin D1	↓	–	–	–	↓	↑	↓
BCL2					Not detected		
Cell viability	–	–	–	–	–	–	–
Cell growth	↓↓	↓	↓	↓↓↓	↓↓↓	↓↓	↓↓↓↓
Growth recovery	↓↓↓	↓	↓	↓↓↓	↓↓↓	↓↓	↓↓↓↓

Note: Effects of combination treatments on cells were compared with those of cells treated with the vehicle DMSO. SAHA/Ra: SAHA combined with rapamycin (Ra); SAHA/LY: SAHA combined with LY294002 (LY); Ra/LY: rapamycin (Ra) combined with LY294002 (LY); SAHA/Ra/LY: SAHA combined with rapamycin (Ra) and LY294002 (LY). ↑: Increased; ↓: reduced; −: no significant change.

class II PI3K is resistant to LY (31, 32). However, LY inhibited growth of the three studied cell lines in a similar pattern, suggesting that p70S6K and 4E-BP1 are main effectors of LY-induced growth reduction.

The mTOR inhibitor rapamycin reduced cell growth by reducing p70S6K and 4E-BP1 activation, consistent with other reports (33). Unlike LY, rapamycin-related AKT activation depends on the PTEN level. In ESS-1 and HESC cells with comparable levels of PTEN, rapamycin increased pAKT^{S437} and pAKT^{T308} levels. In MES-SA cells with PTEN deficiency, rapamycin increased the level of pAKT^{T308}, but reduced that of pAKT^{S437}. The difference in AKT activation might partially explain the higher sensitivity of MES-SA cells to rapamycin than ESS-1 and HESC cells, also shown in other types of cancer cell (23). Analogs or derivatives of rapamycin have been used in clinical therapy, *e.g*. temosirolimus for renal cancer (33). Thus, our data provide a molecular basis for the application of rapamycin analogs in ESS.

AKT activation is known to promote cell survival, however, many studies revealed that AKT inhibition does not induce cell death (30). In our study, LY strongly reduced AKT activation, but increased BCL2 protein expression and did not promote ESS cell death. Likewise, despite reduced expression of pAKT^{T308} in MES-SA cells, rapamycin up-regulated BCL2 expression and did not cause cell death. However, SAHA reduced BCL2 expression and caused ESS death, in spite of enhanced AKT activation in MES-SA cells. This indicates that BCL2 protein, but not activated AKT plays an essential role in ESS cell survival. However, since AKT is estimated to phosphorylate over 9000 diffract proteins in mammalian cells (34), AKT could be involved in some presently unidentified subtle changes related to cell survival.

Lacking cytotoxicity, LY and rapamycin are less efficient than SAHA as monotherapy. However, the combination of SAHA with LY or rapamycin, or even both, improved efficiency *via* targeting the PI3K pathway at multiple levels, consistent with other studies (19). It might amplify positive therapeutic effects *via* synergistic actions and reduce side-effects by neutralizing the adverse effects of each drug. The strong reduction of activated p70S6K and 4E-BP1 were two main synergistic effects observed in our cell lines upon the combination treatments, suggesting these two effectors are responsible for growth reduction.

Although the combination treatments led to stronger growth inhibition than SAHA alone, one should be aware that the effects of SAHA on cell death were not augmented by combination with LY or rapamycin, or both, because of up-regulation of BCL2. Thus, the combination treatments were not superior to SAHA alone with respect to induction of ESS cell death, but were more cytostatic in normal cells. Therefore SAHA alone might be the first choice of therapy for ESS. Due to the heterogeneity of ESS, SAHA with dual

inhibition of PI3K and mTOR is an efficient therapeutic strategy *via* targeting multiple pathways. However clinical confirmation is needed.

In conclusion, we performed a systematic study on the molecular effects of the HDAC inhibitor SAHA and inhibitors of the PI3K and mTOR pathways in ESS and non-metastasic endometrial stromal cells (schematic illustration of the rationale of combination treatments is shown in Figure 9). Our study was only based on cell culture because no animal model is available for ESS, but the findings allow prediction of potential clinical implications of drugs used alone or in combination in ESS therapy. Moreover, due to the specific genetic backgrounds of the two ESS cell lines, this study could be used as a therapy model for other types of cancer with *PTEN* mutation or loss. The AKT activation status could be used as a predictive marker for the drug response in clinical application.

Conflicts of Interest

The Authors declare no conflict of interest.

Acknowledgements

References

1   Geller MA, Argenta P, Bradley W, Dusenbery KE, Brooker D, Downs LS Jr., Judson PL, Carson LF and Boente MP: Treatment and recurrence patterns in endometrial stromal sarcomas and the relation to c-kit expression. Gynecol Oncol *95*: 632-636, 2004.

2   Beck TL, Singhal PK, Ehrenberg HM, Rose PG, Lele SB, Krivak TC and McBee WC Jr.: Endometrial stromal sarcoma: analysis of recurrence following adjuvant treatment. Gynecol Oncol *125*: 141-144, 2011.

3   Moinfar F, Azodi M and Tavassoli FA: Uterine sarcomas. Pathology *39*: 55-71, 2007.

4   Amant F, Woestenborghs H, Vandenbroucke V, Berteloot P, Neven P, Moerman P and Vergote I: Transition of endometrial stromal sarcoma into high-grade sarcoma. Gynecol Oncol *103*: 1137-1140, 2006.

5   Shubassi G, Robert T, Vanoli F, Minucci S and Foiani M: Acetylation: a novel link between double-strand break repair and autophagy. Cancer Res *72*: 1332-1335, 2012.

6   Helman LJ and Meltzer P: Mechanisms of sarcoma development. Nat Rev Cancer *3*: 685-694, 2003.

7   Hrzenjak A, Moinfar F, Tavassoli FA, Strohmeier B, Kremser ML, Zatloukal K and Denk H: JAZF1/JJAZ1 gene fusion in endometrial stromal sarcomas: molecular analysis by reverse transcriptase-polymerase chain reaction optimized for paraffin-embedded tissue. J Mol Diagn *7*: 388-395, 2005.

8 Mariadason JM: HDACs and HDAC inhibitors in colon cancer. Epigenetics *3*: 28-37, 2008.

9 Gan YH and Zhang S: PTEN/AKT pathway involved in histone deacetylases inhibitor induced cell growth inhibition and apoptosis of oral squamous cell carcinoma cells. Oral Oncol *45*: e150-154, 2009.

10 Demicco EG, Torres KE, Ghadimi MP, Colombo C, Bolshakov S, Hoffman A, Peng T, Bovee JV, Wang WL, Lev D and Lazar AJ: Involvement of the PI3K/Akt pathway in myxoid/round cell liposarcoma. Mod Pathol *25*: 212-221, 2011.

11 Friedrichs N, Trautmann M, Endl E, Sievers E, Kindler D, Wurst P, Czerwitzki J, Steiner S, Renner M, Penzel R, Koch A, Larsson O, Tanaka S, Kawai A, Schirmacher P, Mechtersheimer G, Wardelmann E, Buettner R and Hartmann W: Phosphatidy-linositol-3'-kinase/AKT signaling is essential in synovial sarcoma. Int J Cancer *129*: 1564-1575, 2010.

12 Hernando E, Charytonowicz E, Dudas ME, Menendez S, Matushansky I, Mills J, Socci ND, Behrendt N, Ma L, Maki RG, Pandolfi PP and Cordon-Cardo C: The AKT-mTOR pathway plays a critical role in the development of leiomyosarcomas. Nat Med *13*: 748-753, 2007.

13 Hrzenjak A, Moinfar F, Kremser ML, Strohmeier B, Staber PB, Zatloukal K and Denk H: Valproate inhibition of histone deacetylase 2 affects differentiation and decreases proliferation of endometrial stromal sarcoma cells. Mol Cancer Ther *5*: 2203-2210, 2006.

14 Hrzenjak A, Kremser ML, Strohmeier B, Moinfar F, Zatloukal K and Denk H: SAHA induces caspase-independent, autophagic cell death of endometrial stromal sarcoma cells by influencing the mTOR pathway. J Pathol *216*: 495-504, 2008.

15 Hrzenjak A, Moinfar F, Kremser ML, Strohmeier B, Petru E, Zatloukal K and Denk H: Histone deacetylase inhibitor vorinostat suppresses the growth of uterine sarcomas in vitro and *in vivo*. Mol Cancer *9*: 49, 2010.

16 Marks PA and Xu WS: Histone deacetylase inhibitors: Potential in cancer therapy. J Cell Biochem *107*: 600-608, 2009.

17 Perdiz D, Mackeh R, Pous C and Baillet A: The ins and outs of tubulin acetylation: more than just a post-translational modification? Cell Signal *23*: 763-771, 2010.

18 Hubbert C, Guardiola A, Shao R, Kawaguchi Y, Ito A, Nixon A, Yoshida M, Wang XF and Yao TP: HDAC6 is a microtubule-associated deacetylase. Nature *417*: 455-458, 2002.

19 Erlich RB, Kherrouche Z, Rickwood D, Endo-Munoz L, Cameron S, Dahler A, Hazar-Rethinam M, de Long LM, Wooley K, Guminski A and Saunders NA: Preclinical evaluation of dual PI3K-mTOR inhibitors and histone deacetylase inhibitors in head and neck squamous cell carcinoma. Br J Cancer *106*: 107-115, 2011.

20 DePasquale JA, Samsonoff WA and Gierthy JF: 17-beta-Estradiol induced alterations of cell-matrix and intercellular adhesions in a human mammary carcinoma cell line. J Cell Sci *107(Pt 5)*: 1241-1254, 1994.

21 Fantin VR and Richon VM: Mechanisms of resistance to histone deacetylase inhibitors and their therapeutic implications. Clin Cancer Res *13*: 7237-7242, 2007.

22 Song MS, Salmena L and Pandolfi PP: The functions and regulation of the PTEN tumour suppressor. Nat Rev Mol Cell Biol *13*: 283-296, 2012.

23 Steelman LS, Navolanic PM, Sokolosky ML, Taylor JR, Lehmann BD, Chappell WH, Abrams SL, Wong EW, Stadelman KM, Terrian DM, Leslie NR, Martelli AM, Stivala F, Libra M, Franklin RA and McCubrey JA: Suppression of PTEN function increases breast cancer chemotherapeutic drug resistance while conferring sensitivity to mTOR inhibitors. Oncogene *27*: 4086-4095, 2008.

24 Nagata Y, Lan KH, Zhou X, Tan M, Esteva FJ, Sahin AA, Klos KS, Li P, Monia BP, Nguyen NT, Hortobagyi GN, Hung MC and Yu D: PTEN activation contributes to tumor inhibition by trastuzumab, and loss of PTEN predicts trastuzumab resistance in patients. Cancer Cell *6*: 117-127, 2004.

25 Djordjevic B, Hennessy BT, Li J, Barkoh BA, Luthra R, Mills GB and Broaddus RR: Clinical assessment of PTEN loss in endometrial carcinoma: immunohistochemistry outperforms gene sequencing. Mod Pathol *25*: 699-708, 2012.

26 Koul D: PTEN signaling pathways in glioblastoma. Cancer Biol Ther *7*: 1321-1325, 2008.

27 Moinfar F, Kremser ML, Man YG, Zatloukal K, Tavassoli FA and Denk H: Allelic imbalances in endometrial stromal neoplasms: frequent genetic alterations in the nontumorous normal-appearing endometrial and myometrial tissues. Gynecol Oncol *95*: 662-671, 2004.

28 Courtney KD, Corcoran RB and Engelman JA: The PI3K pathway as drug target in human cancer. J Clin Oncol *28*: 1075-1083, 2010.

29 Blay JY: Updating progress in sarcoma therapy with mTOR inhibitors. Ann Oncol *22*: 280-287, 2010.

30 Engelman JA: Targeting PI3K signalling in cancer: opportunities, challenges and limitations. Nat Rev Cancer *9*: 550-562, 2009.

31 Domin J, Pages F, Volinia S, Rittenhouse SE, Zvelebil MJ, Stein RC and Waterfield MD: Cloning of a human phosphoinositide 3-kinase with a C2 domain that displays reduced sensitivity to the inhibitor wortmannin. Biochem J *326(Pt 1)*: 139-147, 1997.

32 Virbasius JV, Guilherme A and Czech MP: Mouse p170 is a novel phosphatidylinositol 3-kinase containing a C2 domain. J Biol Chem *271*: 13304-13307, 1996.

33 Choo AY and Blenis J: Not all substrates are treated equally: implications for mTOR, rapamycin-resistance and cancer therapy. Cell Cycle *8*: 567-572, 2009.

34 Lawlor MA and Alessi DR: PKB/Akt: a key mediator of cell proliferation, survival and insulin responses? J Cell Sci *114*: 2903-2910, 2001.